Probing the Reversibility of Silicon Monoxide Electrodes for Lithium-Ion Batteries

Tan, Tian; Lee, Pui-Kit; Yu, Denis Y. W.

Document Version:
Final Published version, also known as Publisher's PDF, Publisher's Final version or Version of Record

License:
CC BY

Publication record in CityU Scholars:
Go to record

Probing the Reversibility of Silicon Monoxide Electrodes for Lithium-Ion Batteries

Tian Tan, Pui-Kit Lee, and Denis Y. W. Yu [z]

School of Energy and Environment, City University of Hong Kong, Hong Kong

Silicon monoxide is a potential high-capacity anode material for lithium-ion batteries. However, its low initial Coulombic efficiency hinders its adoption in commercial batteries. Here, we use an electrochemical approach, depth of discharge test, to study the origin of the irreversibility in SiO electrodes. We find two contributions to the irreversible capacity of SiO, depending on the reaction products during lithiation. Carbon-coating the material improves the reversible capacity as it increases its electrical conductivity. Disproportionation is an effective way to decrease irreversibility in the initial cycle with the formation of large cluster of SiO_2 which is electrochemically inactive. Though, the reversible capacity is reduced.

Silicon monoxide (SiO) is a promising anode material for lithium-ion batteries (LIBs) with a reversible capacity of more than 1000 mAh g^{-1}, much higher than that of graphite.[1] However, it suffers from two major issues. First, it undergoes a large volume expansion of about 200% during lithiation, which leads to pulverization of the particles and electrode cracking.[2] Second, the material has a low first cycle efficiency (FCE) due to the formation of inactive lithium silicate in the material.[3] Some of the mechanical problems can be suppressed by the reduction of particle size and utilization of a stronger binder.[4] In this study, we investigate the factors affecting the initial reversibility of SiO to develop insights to improve the material.

Previous works indicate that the lithiation of SiO results in the formation of lithium oxide and lithium silicate such as Li_4SiO_4 (mainly), Li_2SiO_5, Li_2SiO_3, as well as lithiated silicon ($Li_{3.75}Si$).[5–7] The material shows low FCE (65.1–82.1%), as the Li-ions are trapped mainly as Li_2O and lithium silicate inside it. The amount of oxygen in SiO_x has been found to be an important factor affecting its FCE - Kim et al. discovered that the increase of oxygen atomic ratio in SiO_x leads to a decrease in FCE,[8] while Yang et al. showed that the reduction of SiO_x by mechanochemical/thermal reduction with Li metal can improve the FCE.[9] Prelithiation by methods such as electrochemical discharging of SiO with Li, direct contact between the SiO electrode and Li metal, and coating Li metal onto the polypropylene separator can increase FCE.[10] However, these methods typically require the use of glove box or dry room for the processing of the Li metal and are not practical for mass production.

To understand and quantify the irreversibility of SiO, we adopted the "depth of discharge" (DOD) test here that we have previously developed to the study of Si electrodes.[11] The detailed procedure of the test can be found in our previous publication, but in brief, electrodes are discharged to different degree of lithiation, and then charged subsequently to monitor the reversible capacity. Here, we first performed the DOD tests on SiO materials to understand the contributions to its irreversibility. Then, the effects of carbon-coating and disproportionation were studied. Amorphous SiO can be disproportionated into nanocrystalline Si domain and SiO_2 cluster above 850°C, thus changing the capacity and efficiency of the material.[12,13]

Experimental

Materials.—SiO and carbon-coated SiO (SiO@C with 3 wt% C) were provided by Osaka Titanium Technologies Co., Ltd., Japan. The Si:O ratio is 1:1.12. All other chemicals were of analytical grade and used as received.

Disproportionation of SiO@C.—Disproportionated-SiO (d-SiO) powders were obtained by thermal treatment. Typically, SiO@C powders were heat-treated in a tube furnace at 900°C (d-SiO@C-900°C) and 1000°C (d-SiO@C-1000°C) under an Argon (Ar) atmosphere for 24 hrs with a heating rate of 5°C min^{-1}. After the annealing process, the furnace was cooled naturally to room temperature.

Material characterizations.—The morphology and structure of the materials were studied by scanning electron microscopy (SEM, Philips XL30FEG). The crystal structure of powders was analyzed by powder X-ray diffraction (XRD, D2 Phaser Brucker) in the 2θ range from 10 to 80° with an acquisition rate of 0.05° per second with Cu K$_\alpha$ radiation ($\lambda = 0.154178$ nm) as the X-ray source. Thermogravimetric analysis (TGA) was performed to determine the Si:O ratio of the material from room temperature to 1000°C with a ramp rate of 10°C min^{-1} in air and hold at 1000°C for 72 hrs.

Electrode fabrication and battery test.—The SiO materials were mixed with acetylene black (AB) (>99.9%, S. A. 75 m^2 g^{-1}, Alfa Aesar, USA) and polyacrylic acid (PAA) (M.W. 450,000, Sigma-Aldrich, Germany) binder with a weight ratio of 6:1:2 by a mortar and a pestle using N-methyl-2-pyrrolidone (NMP, ≥99.5%, MTI, China) as solvent to form slurry. The slurry was then coated onto copper foil using a doctor blade. The electrode was dried on a hot plate and compressed by a roll press, after which the electrode was punched into 16 mm diameter discs. The packing density of all electrodes were adjusted to about 1.2 g cm^{-3}, with electrode loadings of about 1 mg cm^{-2}. This corresponds to an electrode porosity of about 40–50% (see Table I). The electrodes were then dried at 110°C for 4 hours in a Buchi oven before they were transferred into an Ar-filled glove box. The electrodes were assembled into 2032 coin cells with 1 mol L^{-1} LiPF$_6$ in fluoroethylene carbonate (FEC) and diethyl carbonate (DEC) electrolyte with a 1:1 ratio by volume (99.95%, Dodo Chemical, China) as the electrolyte. Lithium metal (99.9%, MTI, China) was used as the counter electrode and Celgard 2325 membrane (Celgard Inc. USA) was used as the separator. Charge/discharge tests of the

Table I. Calculated SiO electrode parameters in this study.

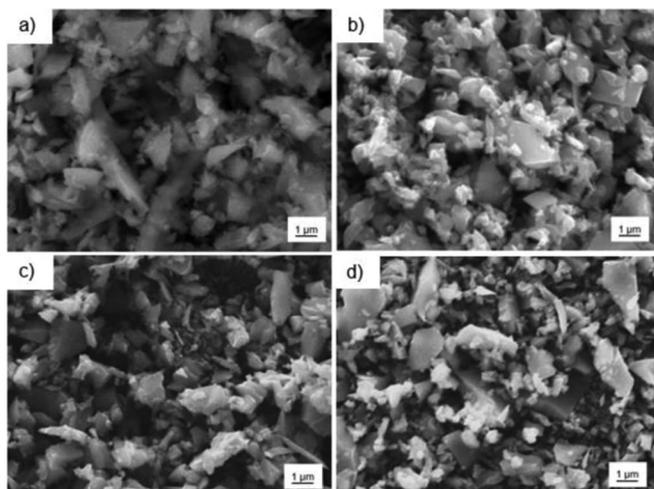| Material	Loading (mg cm^{-2})	Packing density (g cm^{-3})	Porosity (%)
SiO	0.98~1.02	~1.2	44~46
SiO@C	0.95~1.05	~1.2	40~49
d-SiO@C-900°C	0.94~1.00	~1.2	40~48
d-SiO@C-1000°C	0.97~1.07	~1.2	41~47

[z]E-mail: denisyu@cityu.edu.hk

Figure 1. SEM images of a) SiO, b) SiO@C, c) SiO@C disproportionated at 900°C, and d) SiO@C disproportionated at 1000°C.

coin cells were carried out at current rate of 150 mA g^{-1} on a battery tester (Neware, China) between 0.01 and 2 V vs. Li/Li$^+$. For the depth of discharge test (DOD), multiple cells were made and discharged to different capacity limits (i.e. 500, 1000, 1500 mAh g^{-1} and fully lithiated), and then charged to 2 V vs. Li/Li$^+$. Impedance tests were carried out after the electrodes were charged to 1.3 V vs. Li/Li$^+$ with a voltage amplitude of 10 mV between 10 mHz and 100 kHz (Bio-Logic VMP3). All of the battery tests were carried out at 23 ± 1°C. The capacities were calculated with respect to the total mass of the active material.

Results and Discussion

Material characterizations.—Figure 1a displays the SEM image of the pristine SiO particles. The particles are irregular in shape, but the average particle size is about 1 μm. Carbon-coating the material results in material with similar morphology and size (Figure 1b). Figures 1c and 1d show similar appearance of the SiO@C material after disproportionation at 900°C and 1000°C, respectively. These images indicate that the heat-treatment process did not alter the morphology and shape of the materials.

The XRD patterns of pristine SiO, SiO@C, d-SiO@C-900°C, and d-SiO@C-1000°C powders are shown in Figure 2. The SiO material is amorphous, as no crystalline peaks can be observed. Carbon-coated
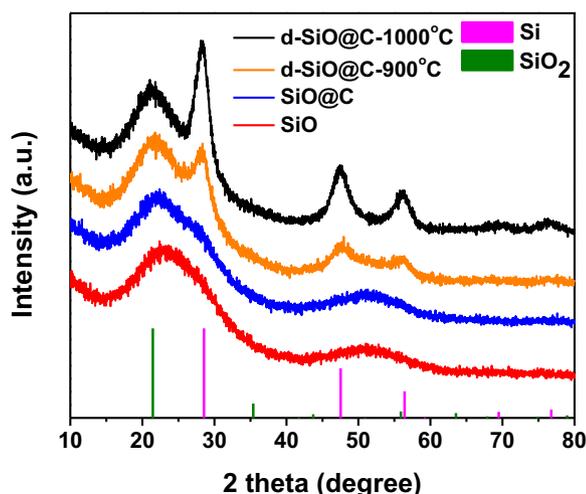

Figure 2. XRD patterns of SiO, SiO@C, SiO@C disproportionated at 900°C and SiO@C disproportionated at 1000°C.
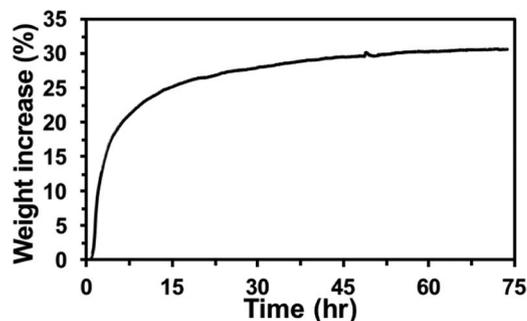

Figure 3. TGA result of SiO sample.

SiO also shows an amorphous structure. In contrast, Si peaks can be observed after 900°C disproportionation and the intensity of the Si peaks increases at higher temperature (1000°C). This suggests that during the high-temperature annealing, SiO is disproportionated into Si and SiO$_2$ regions, similar to that observed by Park et al.[14]

TGA was conducted to obtain the ratio of Si:O in the pristine sample. During the heat-treatment to 1000°C, SiO will react with oxygen in air to form SiO$_2$. According to the TGA data (Figure 3), the weight increase is about 30.5%. This corresponds to a starting material of SiO$_{1.12}$. The Si:O ratio is consistent with that of Hirata et al., where the analyses were carried out on materials from the same source.[12]

Depth of discharge tests on SiO.—SiO powders were first tested to understand the contributions to its discharge and charge capacities. Identical cells were made and discharged to different capacity limits under the DOD test, and then were charged to 2 V vs. Li/Li$^+$. An upper cutoff potential of 2 V vs. Li/Li$^+$ is chosen here as we intend to study the fundamental charge-discharge mechanism of SiO including the investigation of the amount of reversible and irreversible capacities from the conversion reaction (Li$_2$O). Figure 4a shows the 1st discharge and charge curves of the SiO batteries discharged to 500, 1000, 1500 mAh g^{-1} and 0.01 V vs. Li/Li$^+$. Since the first discharge curves for all cells overlapped each other, only the curve corresponding to a full discharge is plotted in Figures 4a–4d and the end points of different cells are marked as "X". SiO shows a slanted 1st discharge profile, which is characteristic of the amorphous SiO and consistent with other works.[5,6,15] We note that the subsequent charge capacity depends on the depth of discharge – a higher charge capacity is obtained when the material is discharged deeper initially. In the charge curves, the slanted region between 0.2 V and 0.65 V vs. Li/Li$^+$ is attributed to the removal of lithium from the Li-Si alloy. The small capacity between 0.65 V and 2 V vs. Li/Li$^+$ is attributed to the partial removal of lithium from Li$_2$O formed during the previous lithiation.

To determine the contributions to the reversible and irreversible capacities, we can plot the initial charge capacity vs. discharge capacity for different cells as in Figure 4e. The data show a linear pattern which can be fitted with a straight line. In addition, the fitted line is deviated from the origin with a non-zero x-intercept. From our previous analysis, the slope of the line represents the intrinsic efficiency of the material, which is the proportion of lithium that can be extracted reversibly from the material.[11] On the other hand, the non-zero x-intercept represents the amount of capacity that is completely irreversible. For the SiO material charged to 2 V vs. Li/Li$^+$ in this work, the measured slope is 80% with an x-intercept of 264 mAh g^{-1} (Table II.) This suggests that on top of an irreversible capacity of 264 mAh g^{-1} during first discharge, an extra 20% of the Li remained in the material after charging to 2 V. If a cutoff potential of 1 V vs. Li/Li$^+$ is considered, as in a practical battery, the intrinsic efficiency (slope) of SiO is reduced to 75%, and the amount of irreversible capacity is increased to 399 mAh g^{-1} because the Li$_2$O component is regarded as irreversible with a lower cutoff potential. Compared to crystalline Si materials, which has an intrinsic efficiency of 90% and an x-intercept
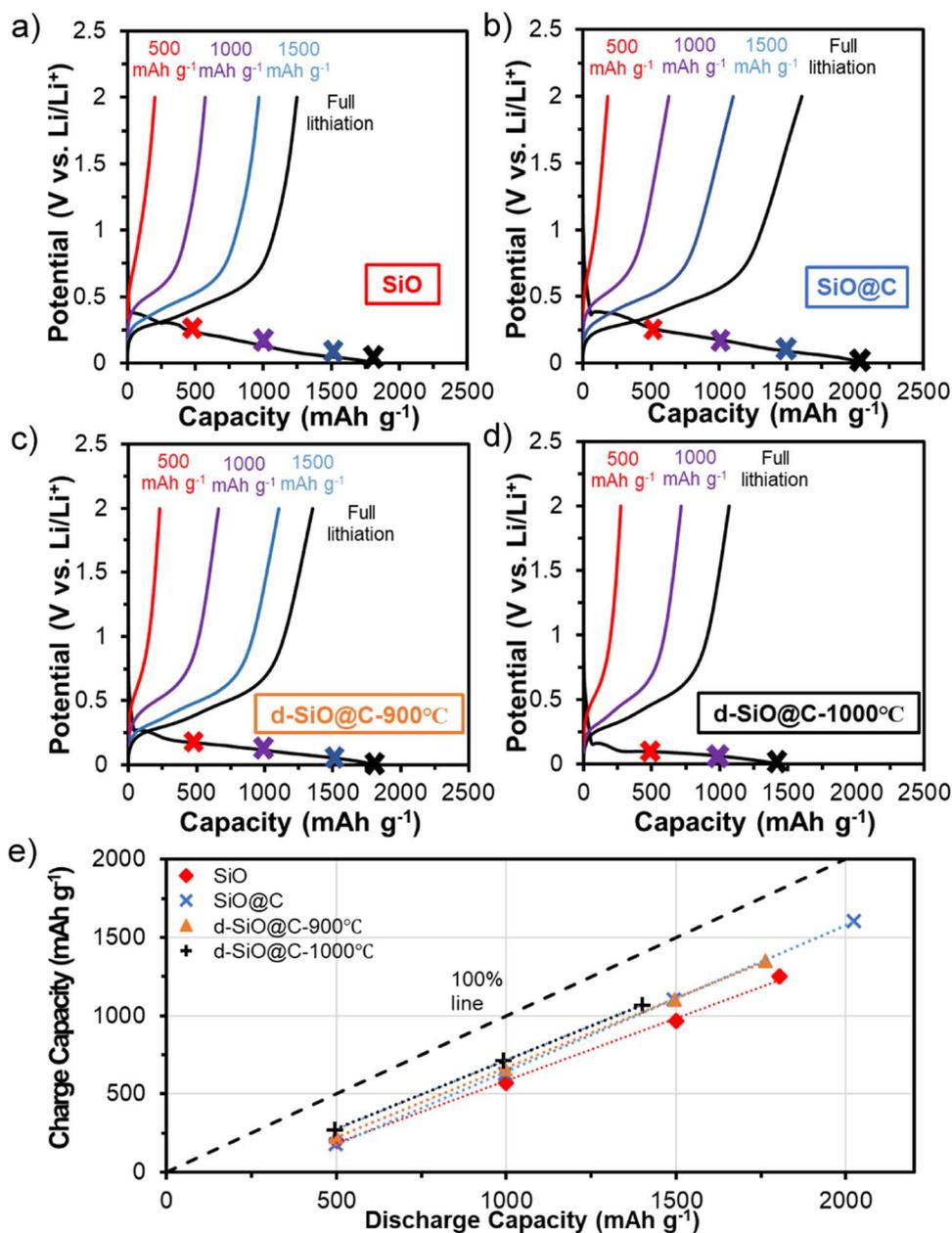
Figure 4. First cycle discharge-charge curves of a) SiO, b) SiO@C, c) d-SiO@C-900°C, d) d-SiO@C-1000°C with different discharge capacity limits, and e) initial charge capacity vs. initial discharge capacity from depth of discharge tests with different electrodes.

of 55 mAh g^{-1},[11] SiO has a much lower intrinsic efficiency (more Li trapped in the material) and a larger irreversible capacity.

Previous work by Kim et al. has suggested that during the lithiation of SiO, $Li_{3.75}Si$, Li_2O and Li_4SiO_4 are formed.[5] Among the reaction products, Li_4SiO_4 is suspected to be completely inactive, whereas Li_2O can be charged and discharged to a certain degree and contributes significantly to the conversion reaction of oxide materials such as NiO, SnO_2, etc.[16,17] These are consistent with results from our DOD test. Our work suggests that there are 2 contributions to the irreversible capacity of SiO: 1) the formation of an inactive matrix of lithium silicate, represented by the x-intercept; 2) the efficiency of the delithiation of $Li_{3.75}Si$ and Li_2O, represented by the slope of the DOD test (see Figure 4e). To further analyze the results, we hypothesize a reaction mechanism during lithiation of SiO as following:

$$SiO_{1.12} + y\,Li^+ + y\,e^- \rightarrow a\,Li_{3.75}Si + b\,Li_2O + c\,Li_4SiO_4 + d\,SiO_2$$
$$[1]$$
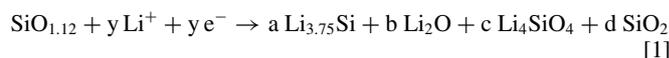
Where "$Li_{3.75}Si/Li_2O$" is partially reversible (with an efficiency given by the slope of the DOD test) and "Li_4SiO_4" is irreversible (corresponding to the x-intercept of DOD test). Capacity corresponding to solid electrolyte interphase (SEI) formation can be included in the coefficient "c" as part of the irreversible component. Since the measured capacity of our SiO sample at full discharge (1804 mAh g^{-1}) is smaller than the theoretical capacity of 2459 mAh g^{-1} (assuming 20% Li_2O product based on Kim et al.[5]), we speculate there is a por-

Table II. Summary of slope and x-intercept from DOD test of SiO, SiO@C and disproportionated SiO@C.
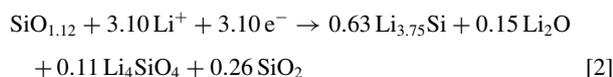
Material	Slope	x-intercept (mAh g^{-1})
SiO	80% ± 0.5%	264 ± 5
SiO@C	93% ± 0.2%	310 ± 4
d-SiO@C-900°C	88% ± 0.2%	246 ± 2
d-SiO@C-1000°C	87% ± 0.1%	189 ± 1

Table III. Estimated amount of products after first lithiation. "a", "b", "c" and "d" are coefficients as given in Equation 1.

Material	a	b	c	d
SiO	0.63	0.15	0.11	0.26
SiO@C	0.67	0.20	0.13	0.19
d-SiO@C-900°C	0.62	0.14	0.10	0.28
d-SiO@C-1000°C	0.54	0.03	0.08	0.38

tion of SiO_2 in the material that are not reacted (4th compound). The compositions of the product "a", "b", "c", and "d" in Equation 1 can be estimated using results from the DOD test. Specifically, the coefficient "c" corresponds to the x-intercept of the DOD test (264 mAh g^{-1}) based on the assumption that Li_4SiO_4 is irreversible. The total first discharge capacity obtained can be converted into the value of "y". The remaining three coefficients can be solved as there are 3 relationships corresponding to the balance of chemical elements of Li, Si and O.
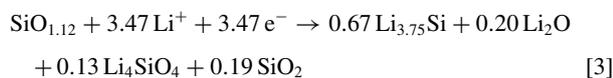
The fitted parameters for SiO based on the obtained 1st discharge capacity and the x-intercept of the DOD test is shown in Table III, and the reaction is estimated to be:

$$SiO_{1.12} + 3.10\,Li^+ + 3.10\,e^- \rightarrow 0.63\,Li_{3.75}Si + 0.15\,Li_2O$$
$$+ 0.11\,Li_4SiO_4 + 0.26\,SiO_2 \qquad [2]$$

The result suggests that for every mole of $SiO_{1.12}$, the products after lithiation are 0.63 moles $Li_{3.75}Si$, 0.15 moles Li_2O, 0.11 moles Li_4SiO_4 and 0.26 moles SiO_2. A total of 3.10 moles of Li^+ is inserted, corresponding to the first discharge capacity of 1804 mAh g^{-1}. The measured first charge capacity is 1250 mAh g^{-1}, corresponding to an extraction of 2.14 moles of Li^+. This is consistent with Equation 2, where 80% (= slope of DOD test) of Li in "$Li_{3.75}Si/Li_2O$" is reversible (i.e. $0.8 \times ((0.63 \times 3.75) + (0.15 \times 2)) = 2.13$), and all Li in Li_4SiO_4 is irreversible. In addition, most of the Li is removed from the $Li_{3.75}Si$ component formed after lithiation, which is also consistent with the charging curve (Figure 4a) where most of the capacity originates from a potential range below 1 V vs. Li/Li$^+$.

Effect of carbon coating.—SiO is coated by a layer of carbon by chemical vapor deposition. The amount of carbon coating is 3 wt%. The SiO@C material was made into electrodes and tested in the same way as SiO. Figure 4b shows the discharge-charge curves during 1st cycle. With carbon coating, both discharge and charge capacities are higher. In particular, charge curves show a larger contribution to capacity above 0.65 V vs. Li/Li$^+$ compared with pristine SiO, which is attributed to extra lithium removal from Li_2O. The SiO@C electrodes were also subjected to DOD test, and the results are summarized in Figure 4e and Table II. Interestingly, carbon coating increases the slope of the DOD line to 93%, suggesting that more lithium can be extracted from the electrode during delithiation. Though, the x-intercept also increases, suggesting that a larger portion of the lithium is trapped in the form of Li_4SiO_4.

By carrying out the same analysis using Equation 1, the composition after lithiation of SiO@C can be estimated from the discharge capacity and the irreversible capacity (x-intercept of DOD). The reaction is estimated to be:

$$SiO_{1.12} + 3.47\,Li^+ + 3.47\,e^- \rightarrow 0.67\,Li_{3.75}Si + 0.20\,Li_2O$$
$$+ 0.13\,Li_4SiO_4 + 0.19\,SiO_2 \qquad [3]$$

Carbon coating increases the amount of lithiated reactants (a, b and c) and decreases the amount of unreacted SiO_2 after discharge (Table III).

To investigate the reason for the higher capacity after carbon coating, electrochemical impedance spectroscopy (EIS) measurement was carried out. All electrodes used for the EIS tests have similar active material loading of about 1.05 mg cm^{-2}. As shown in Figure 5a, the impedance plots consist of a semicircle in high-frequency region
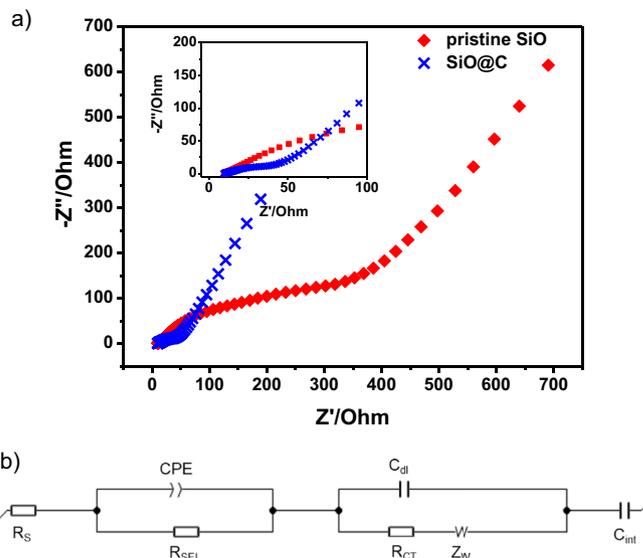
Figure 5. a) Nyquist plots of pristine SiO and SiO@C with enlarged high-frequency region in the inset, and b) equivalent circuit used to fit the experimental data.

which is related to the charge transfer process, and a sloping line in low-frequency region which is ascribed to the solid-state Li diffusion inside active material. These curves are fitted with an equivalent circuit model as given in Figure 5b, where R_S, R_{SEI} and R_{CT} represent the internal resistance, resistance from SEI and charge-transfer resistance, respectively. CPE, C_{dl} and C_{int} are related to constant phase element, double layer capacitance and interaction capacitance, and Z_W is the Warburg resistance corresponding to the lithium diffusion process. It can be seen that carbon coating decreases the charge-transfer resistance (R_{CT}) from 33.8 Ω to 10.7 Ω. These results indicate that the incorporation of carbon layer can significantly improve the electrical conductivity, thus increasing the initial discharge (2024 mAh g^{-1}) and charge capacities.

Carbon coating also increases the slope of the DOD test and the reversible capacity to 93%. This is consistent with the first charge capacity of 1605 mAh g^{-1}, corresponding to an extraction of 2.75 moles of Li from SiO@C. Apart from lithium removal from $Li_{3.75}Si$, we also observe higher reversibility from Li_2O, leading to higher intrinsic efficiency. This is consistent with the additional capacity from a potential above 0.65 V vs. Li/Li$^+$ as seen in the charge curves in Figure 4b.

Effect of disproportionation.—The microstructure of SiO is still controversial. There are two mainstreams of the structural model, one is the random bonding (RB) model and another is random mixture (RM) model.[15,18] The RB model[18] assumes a random network of silicon and oxygen in SiO, while the RM model[15] assumes that there are 2 separate phases including Si and SiO_2. A modified RM model was also proposed by Hirata et al. where SiO acts as a transition layer between amorphous Si and SiO_2.[12] When SiO is heat-treated, it will disproportionate to Si and SiO_2.[13] The amount of crystalline Si and Si^{4+}-based amorphous suboxide will increase as the temperature increases. This is consistent with our XRD results, where the Si and SiO_2 peaks are observed when SiO@C is heat-treated. The peak intensities are higher at higher annealing temperature. Park et al. reported a better FCE and cycle performance with disproportionated SiO (d-SiO).[14] This prompts us to use the DOD test to investigate the effect of disproportionation on the irreversibility of SiO.

The 1st cycle discharge-charge curves for the d-SiO@C-900°C and d-SiO@C-1000°C are shown in Figures 4c and 4d, respectively. With disproportionation, we observe the initial discharge curves shift to lower potential. This is attributed to the discharge of the crystalline
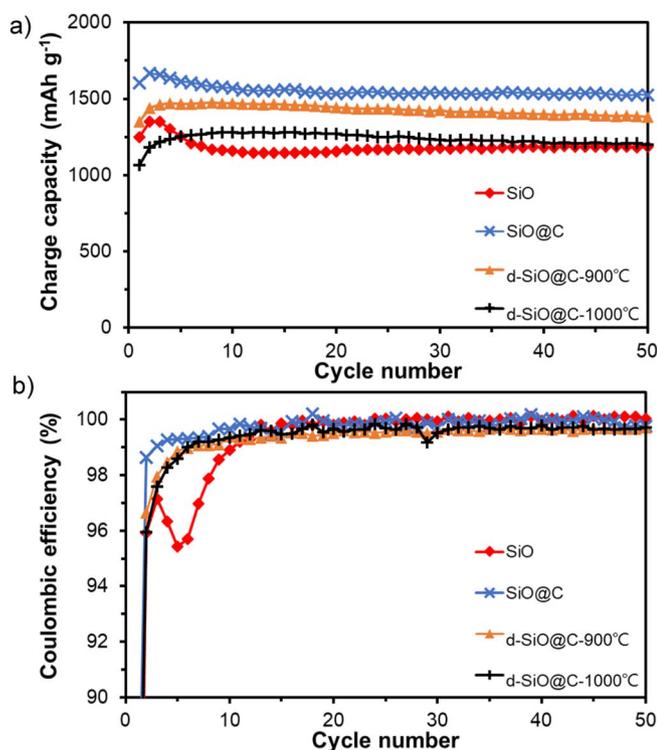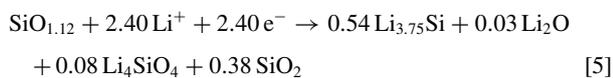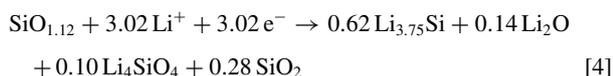
Figure 6. (a) Cycle performance and (b) cycle efficiency of SiO electrodes.

Si that is formed during disproportionation. The initial discharge capacities are also reduced. Interestingly, the results of DOD test give a slope of about 87–88%, while the x-intercepts decrease with disproportionation temperature (Table II).

Using Equation 1 and the respective capacities, the lithiation processes of the d-SiO@C-900°C and d-SiO@C-1000°C after disproportionation can be estimated to be as Equations 4 and 5, respectively:

$$SiO_{1.12} + 3.02\,Li^+ + 3.02\,e^- \rightarrow 0.62\,Li_{3.75}Si + 0.14\,Li_2O$$
$$+ 0.10\,Li_4SiO_4 + 0.28\,SiO_2 \qquad [4]$$

$$SiO_{1.12} + 2.40\,Li^+ + 2.40\,e^- \rightarrow 0.54\,Li_{3.75}Si + 0.03\,Li_2O$$
$$+ 0.08\,Li_4SiO_4 + 0.38\,SiO_2 \qquad [5]$$

The results from the fitting are shown in Table III.

Overall, disproportionation decreases the amount of $Li_{3.75}Si$, Li_2O and Li_4SiO_4 formed after lithiation (coefficients "a", "b" and "c"), but increases the amount of inactive SiO_2 (coefficient "d"). This explains the observed decrease in capacity with disproportionation. This is also consistent with our XRD results and other studies that the amount of Si and SiO_2 is increasing while that of SiO is decreasing as the disproportionation temperature increases.[13,14] Despite a decrease in the amount of lithiated silicide after discharge, the amount of Li_4SiO_4 also decreases, thus increasing the reversibility of the electrode (smaller x-intercept for the DOD test). Disproportionation also decreases the amount of Li_2O formed after discharge, consistent with the lower content of SiO.

Cycle performance of SiO samples.—Cycle performance of the 4 types of electrodes were tested at 150 mA g^{-1}, and the results

are shown in Figure 6. SiO electrode shows a small drop in capacity during the first 10 cycles. Cycle efficiencies during the initial 10 cycles are also lower than SiO@C electrode, suggesting that there are some more Li trapped in the electrode with cycling. SiO@C shows higher charge capacity, better cycle efficiencies and also better cycle performance. Disproportionation decreases the available capacity, with slightly worse cycle performance than the SiO@C material.

Conclusions

We have applied the depth of discharge test to study the contributions to the irreversibility of SiO electrodes. Our results suggest that the amount of irreversible capacity of SiO depends on the type of reaction products. Using the obtained capacities from electrochemical depth of discharge tests, we can estimate the proportion of the reaction products. Even though some simple assumptions have to be made during the analyses, the trends are consistent with our experimental observations. Specifically, carbon coating the material leads to higher reactivity of SiO with Li due to improved electrical conductivity and reversibility of the Li_2O conversion reaction. Though, the amount of inactive lithium silicate is also increased. Disproportionation reduces the irreversibility of SiO by forming some inactive SiO_2 in the material, though the overall capacity is reduced. Our results suggest that there are opportunities to further improve the first cycle efficiency of SiO by finding ways to control the reaction products during initial lithiation process.

ORCID

Denis Y. W. Yu ⓘ https://orcid.org/0000-0002-5883-7087

References

1. C.-H. Doh, C.-W. Park, H.-M. Shin, D.-H. Kim, Y.-D. Chung, S.-I. Moon, B.-S. Jin, H.-S. Kim, and A. Veluchamy, *J. Power Sources*, **179**, 367 (2008).
2. M. Miyachi, H. Yamamoto, H. Kawai, T. Ohta, and M. Shirakata, *J. Electrochem. Soc.*, **152**, A2089 (2005).
3. Z. Wang, Y. Fu, Z. Zhang, S. Yuan, K. Amine, V. Battaglia, and G. Liu, *J. Power Sources*, **260**, 57 (2014).
4. H. Huang, *Int. J. Electrochem. Sci.*, 8697 (2016).
5. J.-H. Kim, C.-M. Park, H. Kim, Y.-J. Kim, and H.-J. Sohn, *J. Electroanal. Chem.*, **661**, 245 (2011).
6. S. C. Jung, H.-J. Kim, J.-H. Kim, and Y.-K. Han, *J. Phys. Chem. C*, **120**, 886 (2016).
7. T. Kim, S. Park, and S. M. Oh, *J. Electrochem. Soc.*, **154**, A1112 (2007).
8. M. K. Kim, B. Y. Jang, J. S. Lee, J. S. Kim, and S. Nahm, *J. Power Sources*, **244**, 115 (2013).
9. X. Yang, Z. Wen, X. Xu, B. Lin, and S. Huang, *J. Power Sources*, **164**, 880 (2007).
10. S. W. Hwang and W. Y. Yoon, *J. Electrochem. Soc.*, **161**, A1753 (2014).
11. P.-K. Lee, Y. Li, and D. Y. W. Yu, *J. Electrochem. Soc.*, **164**, A6206 (2017).
12. A. Hirata, S. Kohara, T. Asada, M. Arao, C. Yogi, H. Imai, Y. Tan, T. Fujita, and M. Chen, *Nature Commun.*, **7**, 11591 (2016).
13. M. Mamiya, M. Kikuchi, and H. Takei, *J. Cryst. Growth*, **237–239**, 1909 (2002).
14. C.-M. Park, W. Choi, Y. Hwa, J.-H. Kim, G. Jeong, and H.-J. Sohn, *J. Mater. Chem.*, **20**, 4854 (2010).
15. G. W. Brady, *J. Phys. Chem.*, **63**, 1119 (1959).
16. U. Boesenberg, M. A. Marcus, A. K. Shukla, T. Yi, E. McDermott, P. F. Teh, M. Srinivasan, A. Moewes, and J. Cabana, *Sci. Rep.*, **4**, 7133 (2014).
17. X. W. Guo, X. P. Fang, Y. Sun, L. Y. Shen, Z. X. Wang, and L. Q. Chen, *J. Power Sources*, **226**, 75 (2013).
18. H. R. Philipp, *J. Non-Cryst. Solids*, **8–10**, 627 (1972).